International Journal of Energy and Power Engineering
2015; 4(5-1): 1-11
Published online August 31, 2015 (http://www.sciencepublishinggroup.com/j/ijepe)
doi: 10.11648/j.ijepe.s.2015040501.11
ISSN: 2326-957X (Print); ISSN: 2326-960X (Online)

CFD Analysis of Effects of Surface Fouling on Wind Turbine Airfoil Profiles

Sashank Srinivasan[1], Vikranth Kumar Surasani[2]

[1]Department of Mechanical Engineering, Birla Institute of Technology and Science-Pilani, Hyderabad Campus, India
[2]Department of Chemical Engineering, Birla Institute of Technology and Science-Pilani, Hyderabad Campus, India

Email address:

sashank.srinivasan.13@gmail.com (S. Srinivasan)

To cite this article:

Sashank Srinivasan, Vikranth Kumar Surasani. CFD Analysis of Effects of Surface Fouling on Wind Turbine Airfoil Profiles. *International Journal of Energy and Power Engineering*. Special Issue: Energy Systems and Developments. Vol. 4, No. 5-1, 2015, pp. 1-11.
doi: 10.11648/j.ijepe.s.2015040501.11

Abstract: One of the important factors that determine the long term efficiency of wind turbine blades is the extent to which the surface finish has been altered from the original state. This can happen either through corrosion or through impingement of particles. This paper aims at analyzing the effect of the later phenomenon on two specific profiles: the NREL S814 and NREL S826 profiles, at different Reynold's numbers. These are two very similar profiles in utility and shape but differ in their thickness. This fact is used to ascertain the effect that thickness of an airfoil has on preventing surface fouling based performance degradation. Surface fouling has been modeled as a roughness at the leading edge of the profile. This is assumed to cause enough flow transition so as to simulate roughness over the entire profile. CFD simulations have been used to perform the analysis and initial results have been validated with experimental data. The accuracy of turbulence models in predicting normal and surface fouled conditions has been assessed. The performance parameters that have been considered are the lift, drag, moment coefficients and the drag to lift ratio.

Keywords: Surface Fouling, Wind Turbine Blades, S814 Airfoil, S826 Airfoil

1. Introduction

To ensure smooth, unseparated flow over wind turbine blades, a great amount of care is taken to obtain a smooth surface finish. However, wind turbines generally operate in harsh environments which causes the surface finish of the blades to deteriorate. This is especially true for off shore marine wind turbines where the flow velocities are much higher than land based windmills. However, this is not the only mode of deterioration of surface finish of the blades. Over a period of use, the blades are impinged with particles from various sources. Some common sources are icing, insects and dust. This is an equally important, if not more worying cause of surface finish deterioration. In the case of corrosion, improvement of blade materials can reduce the damage caused. However, surface fouling is a completely external factor that has to be dealt with during the design process itself. This study makes an attempt in trying to identify airfoil properties, in particular the thickness of airfoil profiles, on mitigating the performance reduction generally associated with surface fouling. Two specific airfoil shapes: the S814 and S826, both designed at NREL, USA, have been considered in this study. The characteristic features of the two profiles are shown in Table 1.

Table 1. *Features of the Airfoils considered.*

Airfoil	Location of use on the blade	Thickness	Design Reynold's Number	Rotor Diameter	Salient Features
S814	Root	24%	$1.5x10^6$	20-30m	High-Lift airfoil
S826	Tip	14%	$1.5x10^6$	20-40m	High-Lift Airfoil

The presence of roughness alters the aerodynamic performance of the profiles. The lift coefficients decrease while the drag increases. These are caused due to increased severity of flow separation as well as transition from laminar to turbulent flow happening at a much earlier upstream location along the profile.

To see the difference in performance due to surface fouling, aerodynamic performance data of a smooth airfoil is required

first. This, as well as other ensuing analyses have been done using a 2 dimensional model of the airfoils in ANSYS Fluent. The mesh generation was performed in ICEM-CFD.

Additionally, various turbulence models were tested out to determine their effectiveness in predicting normal and surface fouled conditions. To simulate surface fouling effects, it is assumed that a roughness specified at the leading edge of the airfoil is sufficient. No matter how much roughness is present on the surface, once the flow has transitioned to turbulent or separated from the surface, the effect of roughness becomes negligible.

2. Methodology Followed

To maintain uniformity while analyzing the airfoils, the flow domain, chord length, fluid considered, inlet velocity and meshing strategy were all held constant.

3. The Flow Domain

A square flow domain was considered to simulate the flow around the airfoils. To ensure infinity boundary conditions at the edges of the flow domain, the boundaries must be sufficiently far away from the airfoil. The norm followed in the current work is to maintain all boundaries at 40 chord lengths away from the airfoil. Since the chord length used is 1m, an 80m X 80m domain, with the airfoil at the center, was used to study the airfoil performance.

4. Grid Generation

Based on coordinates of the points on the airfoils provided by NREL, a CAD model was prepared in Pro/ ENGINEER using a single spline curve connecting all the points. The grid topology used in ICEM-CFD was H-Type for the flow domain while an O-grid was used to mesh the region immediately near the airfoil. The O-grid helps resolve the boundary layer formed over the airfoil accurately. This was ensured by constructing meshes with y+ values less than 1. This means that the boundary layer does not remain within one single element of the mesh and hence the boundary layer features of the flow are completely resolved. 100 elements were used in the O-grid surrounding the airfoil. 65 elements were used upstream of the airfoil and 150 elements downstream of the airfoil. In total 235,000 elements were used.

Before continuing with the calculations, a mesh independency study was performed to check if the results do not vary with change in mesh element count. A coarse mesh with 150,000 elements and a fine one with 330,000 were used, apart from the eventual 235,000 element mesh, to simulate the flow around the smooth S814 airfoil at an Angle of Attack (AoA) of 0°. During the process of making the mesh coarser and finer, the y+ value was maintained at values lesser than 1 to ensure accurate results. The lift and drag coefficients were monitored to check if significant variations were predicted by the three meshes. Results for the lift and drag coefficients did not vary by more than 10^{-3} and 10^{-5} units respectively and hence it was concluded that the results were independent of the mesh used. Ultimately, the intermediate mesh size was chosen so as to ensure sufficient mesh density while ensuring computation time remained manageable.

The resulting mesh for the S814 airfoil is shown in Figure 1. The roughness that was specified at the leading edge was restricted to region on the airfoil between the two red lines. A similar mesh was created for the S826 airfoil without any changes in the mesh structure, barring those due to the change of airfoil shape.

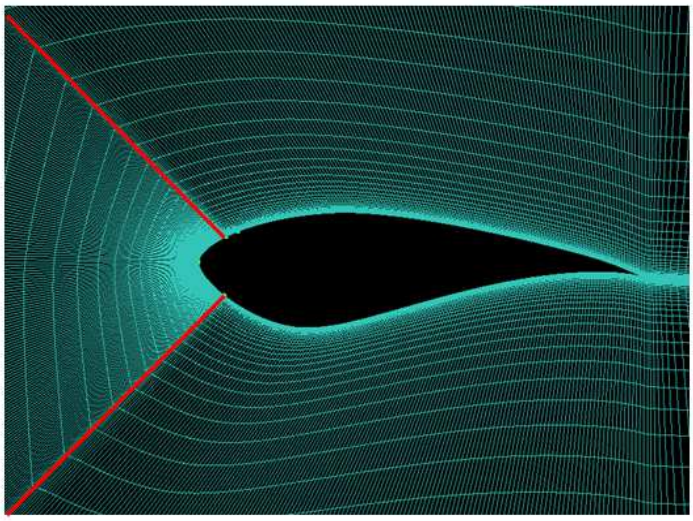

Figure 1. *Grid used for the CFD runs of S814 airfoil.*

5. The Solver: ANSYS Fluent

The popular commercial code: Fluent, was used to perform the CFD calculations. The 2-D, double precision solver was chosen for this study. The fluid considered was incompressible air at atmospheric conditions. Boundary

conditions specified were: No slip boundary at the surface of the airfoil and free shear flow at the upper and lower boundaries of the flow domain. The inlet velocity specified was based on the Reynold's number analyzed. A turbulence intensity of 5% was specified at the inlet. The outlet was assumed to remain at atmospheric pressure due to the far-field boundary assumption. For the present study, the steady state solver was used. The angle of attack was thus limited to the rang: -4° to 10°, after which flow separation effects play a much larger role and the entire flow field becomes unsteady in nature. Residual limits were set at 10^{-6}, although generally residuals were in the range of 10^{-10} when the simulation was deemed converged. The CFD analysis made use of two turbulence models: the 4 Equation Transition SST model and the fully turbulent SST k-ω model. To answer the question of which model predicted which case better, a separate study was made before the start of the proposed analysis using experimental data taken from literature. Details of this study are given in the next sections.

6. Specifying the Roughness

Given that the roughness was considered only at the leading edge, the height and density of the roughness must be such that the flow is immediately transitioned into the turbulent state.

Kerho and Bragg [3] advocate a Reynold's number of at least 600, calculated based on the height of the rough element. For the case of flow Reynold's number of $1.5x\ 10^6$ over the airfoil of chord length 1m, the minimum height of the rough element must be at least 0.4mm. However, if the inlet Reynold's number changes, the required minimum height would also change. To avoid this, specifying a much higher value would be prudent. The value chosen was 1.9mm for the reason that experimental data for S814 airfoil with leading edge thickness elements of the same height were reported in [2]. This data could be used to ascertain the accuracy of predictions by the CFD solver when using different turbulence models. The experimental data was for roughness elements spread over a length of 102mm over a 457mm chord length airfoil. Following the same dimensional ratio, roughness was specified over a length of 220mm, spread over the top and bottom surface of the airfoil. This norm was followed both the airfoils and at all Reynold's numbers analyzed.

7. Turbulence Modelling

The choice of turbulence model is dictated by the type of flow present in the domain and over the airfoil. For the smooth airfoil case, the flow conditions could be laminar over the initial part of airfoil and then transition to turbulent state. If the flow velocity is high enough, the flow could be turbulent right from the leading edge region. There is no definitive way of stating which conditions prevail, although chances of the former occurring are higher. For the rough airfoil, the roughness height specified was high enough to trip the boundary layer and cause immediate transition to turbulence. Here it is possible to state with more confidence that the flow over the airfoil will be fully turbulent.

A definitive check of flow transition is to plot the skin friction coefficient along the surface of the airfoil. The region where there is a sharp dip and then a sudden increase in the skin friction value denotes the location of the transition point. The reason for this is the mechanism of transition to turbulence. During the transition process, the flow momentarily separates from the surface, forming a separation bubble after which the flow reattaches to the surface of the airfoil as a fully turbulent one. The momentary loss of contact between the fluid and the surface causes the skin friction coefficient to drop to zero over a small part of the airfoil. To see this drop and increase, the transition model has to be used. The fully turbulent model assumes that the flow has already transitioned and hence will not predict this behavior.

For the current study, the 4 equation SST transition model with the k-ω-γ-Re_θ correlation implemented by Menter and Langtry [6] and the SST k-ω model were used. The k-ω class of models resolve the boundary layer without the need for any wall functions and have generally been very accurate in airfoil CFD predictions. Both these modes have been used to simulate smooth and rough S814 airfoil. The predictions of lift, drag, moment coefficients along with the lift to drag ratios were compared with experimental data to see which model to use for each of the two cases. This information has then been used to predict the behavior of the S826 airfoil. The moment has been calculated at 25% of chord length.

8. Validation of Turbulence Models with S814

Experimental testing of the S814 airfoil in smooth and surface fouled conditions were conducted by Ferrer and Mandate [2]. This data was used to validate the accuracy of predictions by the SST-Transition and the SST k-ω models at the design Reynold's number. The lift, drag and drag to lift ratio were compared in this regard. Figures 2-7 show the comparison between the predictions.

From the plots shown, it was deduced that the Transition model predicted the smooth airfoil case better than the fully turbulent SST k-ω model. The rough airfoil predictions by both the models in consideration were not so conclusive.

For the rough S814, the transition model predictions of lift were better while the drag and drag to lift ratio predictions by the fully turbulent model were more accurate. However, on the account that the drag to lift ratio takes into account both the forces, the fully turbulent model was slightly better. Furthermore, the moment about $1/4^{th}$ chord length was calculated. This gave a good comparison about how the models predict the distribution of forces over the airfoil.

Figure 8 shows that the fully turbulent SST k-ω model predicts the distribution of forces over the airfoil slightly better than the transition model. Additionally, the transition

location was determine for the rough airfoils. The skin friction coefficient was plotted against chord length to locate the point of transition of the flow. For most Angle of Attacks, transition happens at around 7% side chord length on the upper surface and 5% on the lower side, which are both within the rough region of the leading edge.

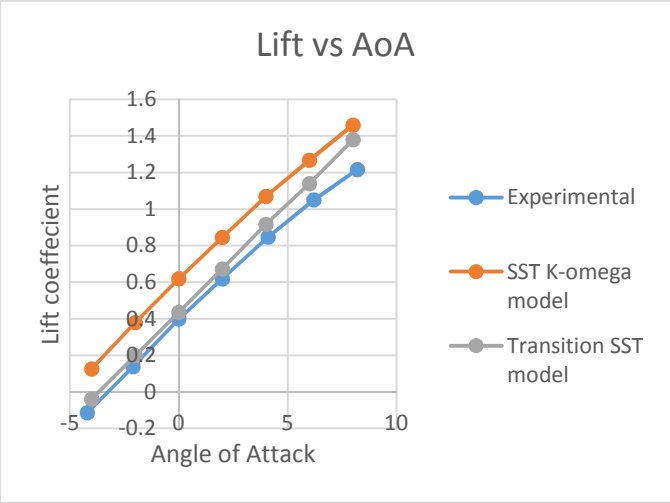

Figure 2. *Variation of lift with angle of attack for S814 (smooth case).*

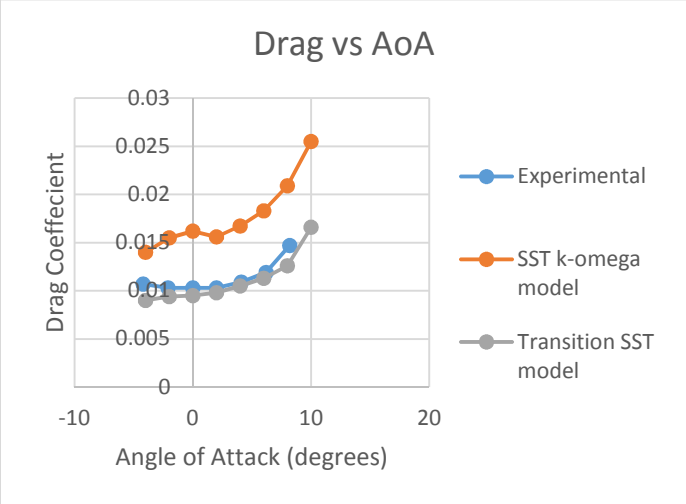

Figure 3. *Variation of lift with angle of attack for S814 (smooth case).*

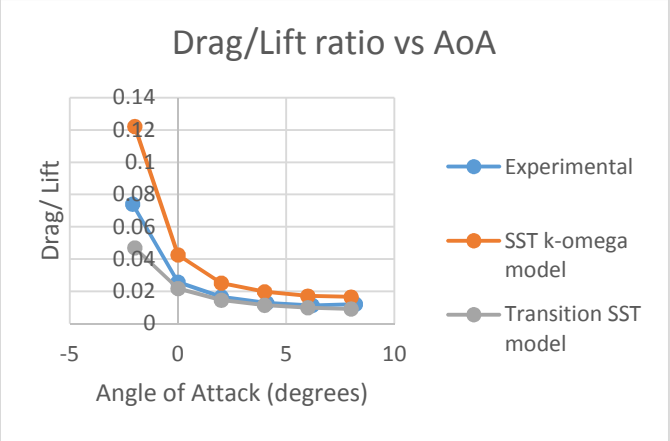

Figure 4. *Variation of drag to lift ratio with angle of attack for S814 (smooth case).*

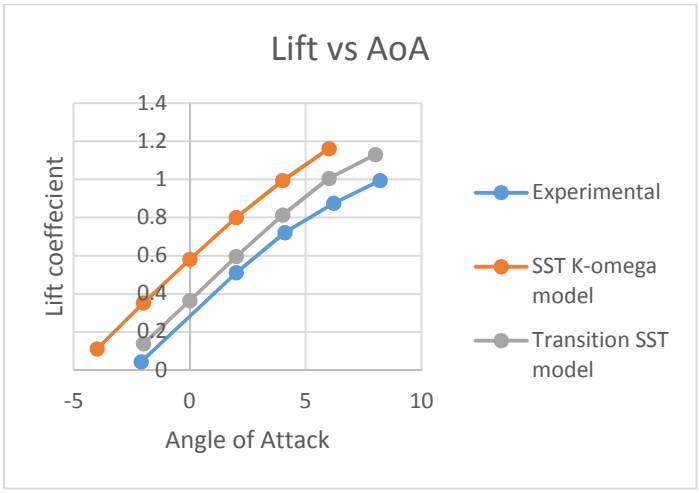

Figure 5. *Variation of lift ratio angle of attack for S814 (rough case).*

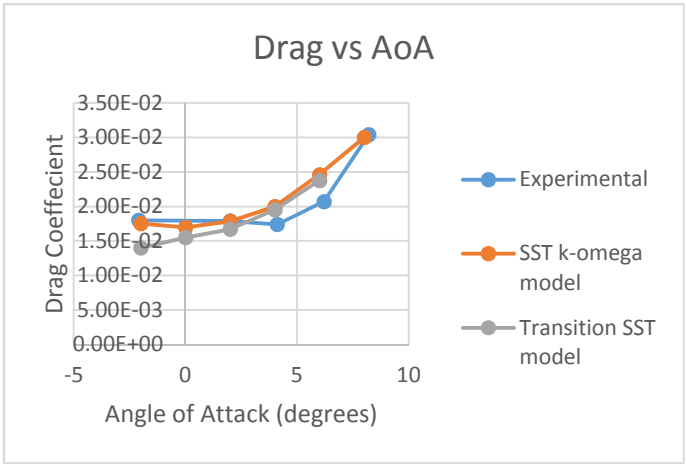

Figure 6. *Variation of drag with angle of attack for S814 (Rough case).*

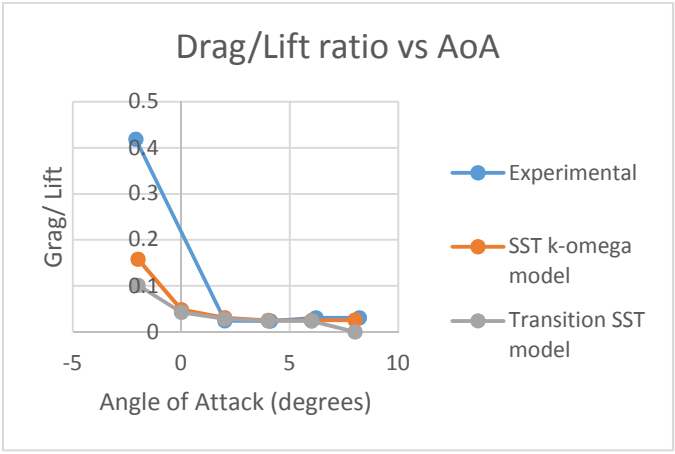

Figure 7. *Variation of drag to lift ratio with angle of attack for S814 (rough case).*

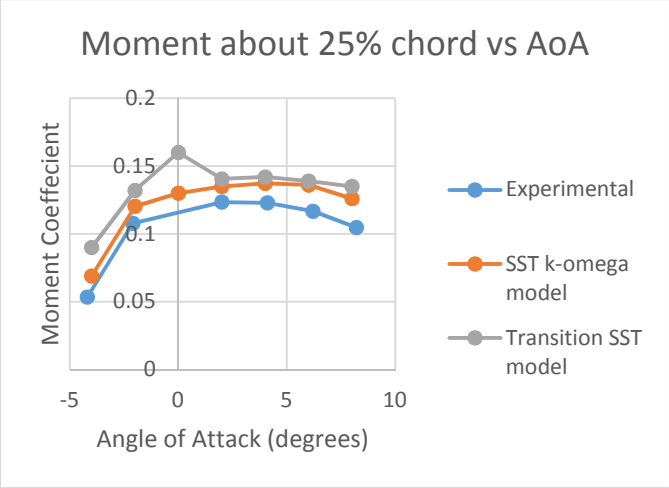

Figure 8. *Variation of moment with angle of attack for S814 (Rough case).*

This confirms that transition does happen within the rough region itself and the height of the rough elements are sufficient to effectively mimic surface fouled conditions. This also shows why the transition model fails, as the flow over more than 90% of the airfoil is fully turbulent.

However, it was still desirable to see if the two airfoils were resistant to the effects of surface fouling at any angle of attack and inlet velocity, even a small way. The lift, drag and moments will obviously deteriorate due to the roughness specified. However, if the transition to turbulent state happens outside the leading edge region of the airfoil, it would show that the airfoil at those operating conditions is relatively more resistant to the harm done by the fouling of the surface. Since this can be predicted only by the transition model, both the models were employed for the rough airfoil scenario. All performance data for rough airfoils were taken from the fully turbulent model only. Smooth airfoils were analyzed only by the transition model as no advantages are brought to the table by the fully turbulent model.

9. Results and Discussion

Having ascertained the turbulence models that are best suitable for the two operating scenarios, the S814 and the S826 airfoils were analyzed at Reynold's numbers of $1.5x\ 10^6$ and $7.5x\ 10^5$. The performance degradation was analyzed trough the change in lift, drag and moment coefficients. Additionally the drag to lift ratio was also monitored. The changes in these parameters were compared in terms of modulus percentage change from the smooth airfoil case. Within the data generated, two major factors that can affect the change in performance are the thickness and the Reynold's number. For ascertaining the effect of thickness in performance degradation, the S814 and S826 were contrasted against each other at both Reynold's numbers which have been considered. For determining the effect that Reynold's number has, the analysis was done by comparing the data of the same airfoil in the two operating conditions.

10. Effect of Reynold's Number

The two profiles were each tested at their design Reynold's number of $1.5x\ 10^6$ and at half that value to see if any improvement or further deterioration of performance takes place.

The change in performance characteristics of S814 airfoil are plotted in figures 9 through 12. The change in lift and moment coefficients remain the same at both Reynold's numbers. The change in drag increases slightly at the higher Reynold's number but the trends in the change is same. This increase in the drag variation from smooth to rough case can be attributed to increased turbulence at higher velocities which magnify on encountering the rough leading edge. Even this increase is at best 10-15% in the main operating range. To a large extent, the performance deterioration does not seem to be affected by the Reynold's number. This means that whatever the velocity of the flow over the turbine blade, once the surface fouling has occurred, there is no possibility of finding alternate optimum velocities through which the performance reduction can be mitigated.

The S826 airfoil was also analyzed in a similar manner. The performance changes are shown in Figures 13-16. Although the drag changes are more pronounced than in the case of S814, the variation in lift and moment remain the same. This further proves the above conclusion. This means that that the surface fouling effects can be reduced to a large extent by better airfoil designs only. The increased sensitivity to Reynold's number change in drag variation of S826 gives an opportunity for designers to optimize based on inlet velocity. In both cases, the drag to lift change is much higher than the change in drag. This is due to the effect of combining the changes in drag and lift.

Another observation from the plots is that the change in the performance parameters reduces as the angle of attack increases. This can be attributed to the already degraded state of the flow in the smooth conditions. At higher AoA, flow separation effects are more predominant in any scenario. The

introduction of a rough leading edge can only do a little more in disturbing that flow field further.

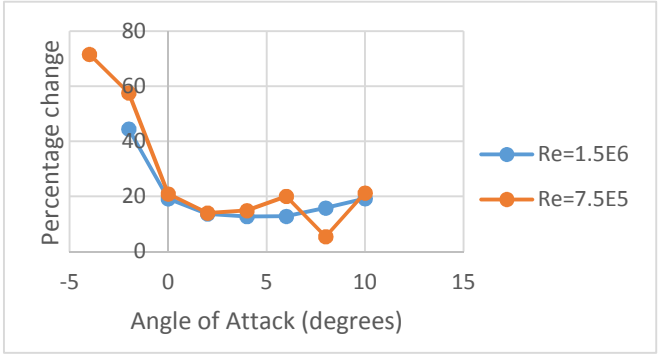

Figure 9. *S814-Change in lift coefficient.*

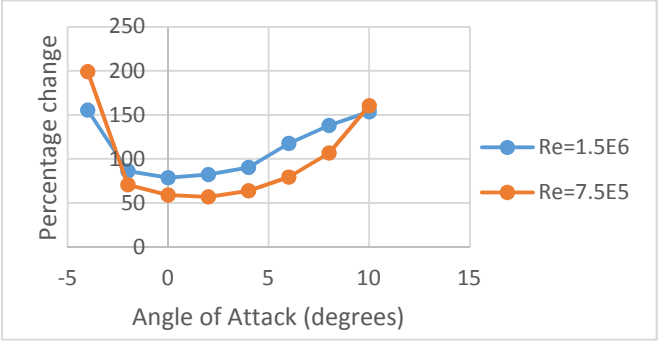

Figure 10. *S814-Change in drag coefficient.*

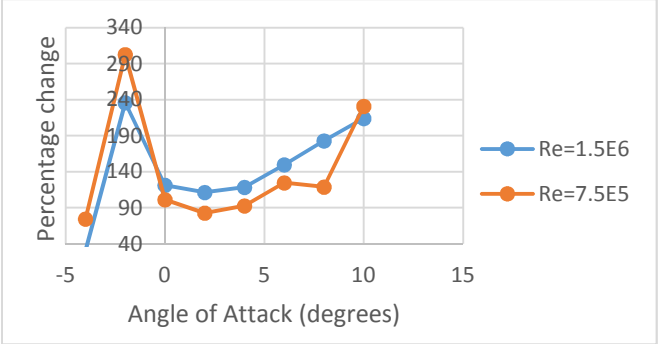

Figure 11. *S814-Change in drag to lift ratio.*

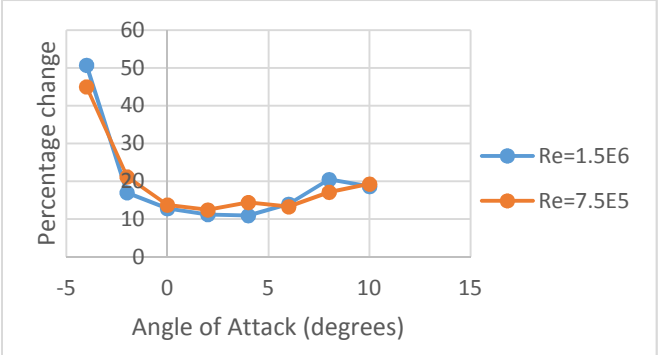

Figure 12. *S814-Change in moment coefficient.*

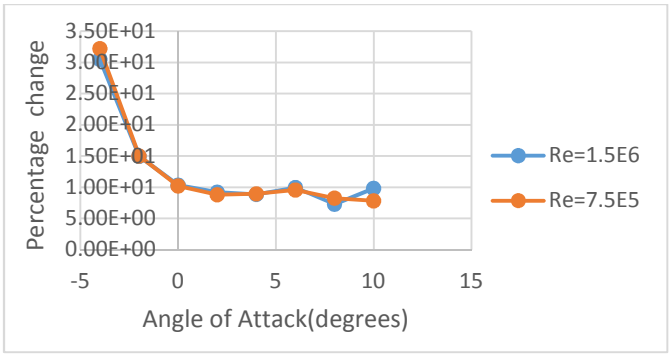

Figure 13. *S826-Change in lift coefficient.*

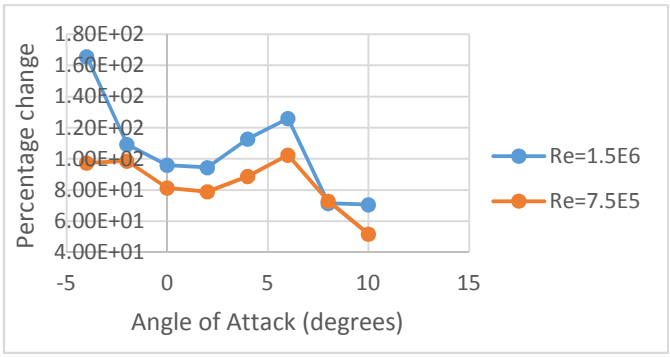

Figure 14. *S826-Change in drag coefficient.*

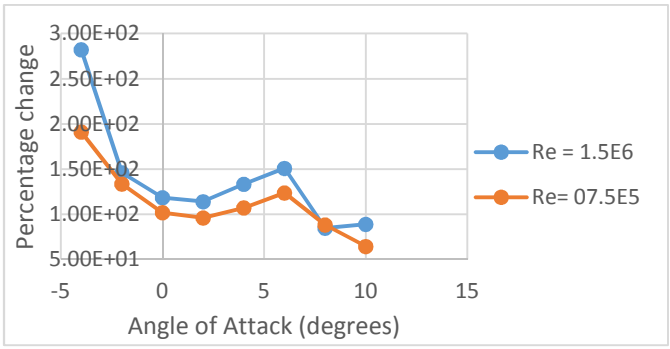

Figure 15. *S826-Change in drag to lift ratio.*

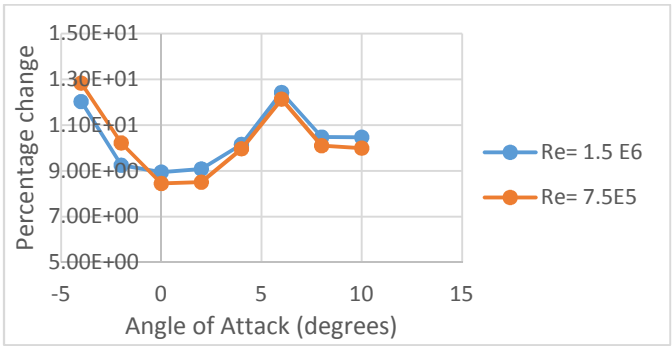

Figure 16. *S826-Change in moment coefficient.*

11. Effect of Thickness on Performance Degradation

The fact that the inlet velocity does not affect the variation in aerodynamic performance means that the deterioration is affected to a major extent by the airfoil properties. The thickness of an airfoil is the focus of the current study. The S814 has a thickness of 24% while the S826 is thinner with a thickness of 14%. This means that the S814 has a maximum thickness of 24% of the chord while the S826 has a

maximum thickness of 14% of the chord length. Since Reynold's number does not affect the change in lift, drag and moment, the effect of thickness was studied at the design Reynold's number only. The conclusions that arise out of this study will thus hold for analysis at any inlet velocity.

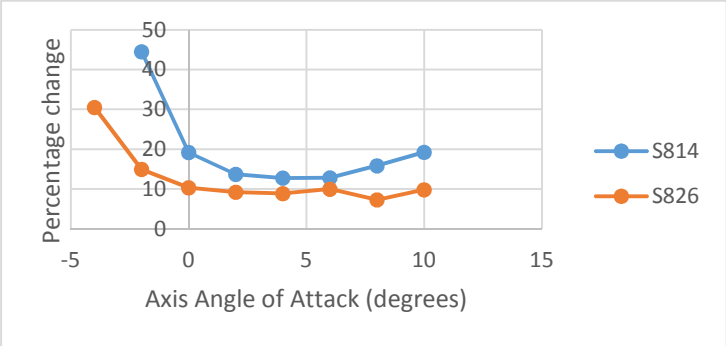

Figure 17. *Comparison of change in Lift.*

With regard to lift force change, the S826 is less affected when compared to the S814. In the case of drag force variation, both the airfoils remain equally affected. At higher angles of attack, the S826 is drastically less affected than the S814, meaning that the S826 is much more stable in surface fouled conditions.

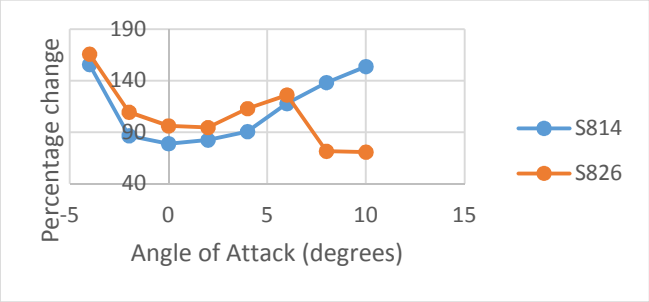

Figure 18. *Comparison of change in Drag.*

The moment coefficient variation is the same for the both the airfoils, except at the extremes of the AoA range considered where the S826 once again outperforms the S814. With a larger picture in mind, the moment coefficient variation is similar to lift. Considering the fact the lift and moment coefficient varied by the same order magnitude while the drag varied by higher margins, a trend is seen in the relationship between lift and moment coefficient changes.

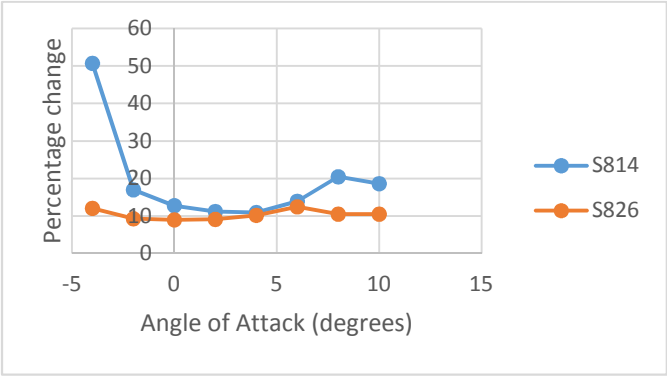

Figure 19. *Moment coefficient variation comparison.*

From the above comparison, the S826 seems to be better suited to tackle suraface roughness. The lift and moment coefficient variation is lesser than the S814 while the drag variation remains the same. However, it was seen that the S826 had the possibility of optimising drag based on Reynold's number and thus the thinner airfoil has an edge over the thicker one in this aspect as well.

The thicker airfoil is more prone to lift and moment based degradation. Within the range of AoA from 0° to 6°, the perfromance variation is almost the same for the moment variation. However at higher angles, the thicker airfoil becomes much more intensely afected. From this, it can be concluded that the S826 airfoil is a more resistant to surface fouling induced perfromance reduction than the S814 airofil.

12. Change in Transition Location

The height of the roughness elements has been specified large enough to cause immediate transition of flow from laminar to turbulent phase in normal flow conditions. However, it was prudent to check if the two airfoils were resistant to this transition at any angle of attack. This analysis was done using the results from the SST transition model. To determine the transition point, a plot of the skin coefficient is used. An example of this is shown in Figure 20. In this particular example, the transition happens at approximately 50% of the chord on the upper surface of the airfoil and at 25% on the lower surface of the airfoil.

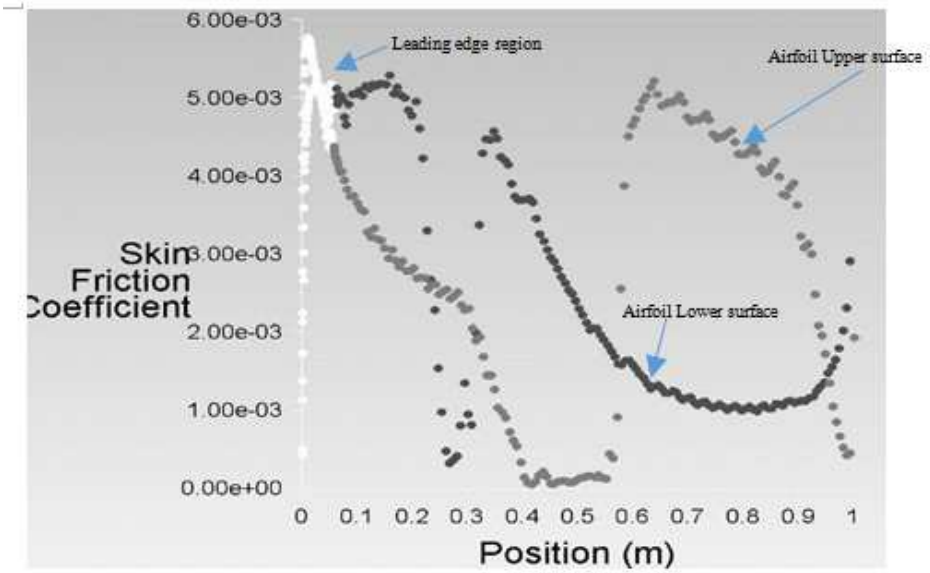

Figure 20. *Plot of skin friction.(S814, smooth, -2° AoA, Re=* $1.5x\ 10^6$*).*

A similar analysis was done for the two airfoils at both the reynold's number analyzed in this study. Both the airtfoils were unable to negotiate the ill effects of the leading edge roughness element and the transition occurred within the leading edge region only.

13. Conclusions

The S814 and S826 airfoils were analyzed at two Reynold's numbers of $1.5x\ 10^6$ and $7.5x\ 10^5$. Transitional and fully turbulent models were assessed based on accuracy of predicting normal and rough airfoils using experimental data of S814. It was observed that the transition model predicted flow over smooth airfoils better while the fully turbulent model predicted surface fouled conditions more accurately.

The performance of the two airfoils were compared between normal operating conditions and surface fouled conditions. For both the airfoils, the Reynold's number did not play a major role in mitigating or worsening of aerodynamic performance during surface fouled conditions. Additionally, it was observed that the thinner S826 airfoil was more resistant to surface fouling induced performance degradation than the S814 airfoil. The location of the transition point was analyzed to see if at some angle of attack, the airfoils were able to prevent immediate transition at the leading edge. Both airfoils failed in preventing fully turbulent flow from happening over the entire airfoil.

References

[1] Dalili.A, Edrisy.A, Carriveau.R, 2009 "A review of surface engineering issues critical to wind turbine performance", Renewable and Sustainable Energy Reviews 13, pp. 428–438

[2] Ferrer.E ,Munduate.X, 2009, "CFD predictions of transition and distributed roughness over a wind turbine airfoil", 47th AIAA Aerospace Sciences Meeting Including The New Horizons Forum and Aerospace Exposition.

[3] Kerho.M.F, Bragg.M.B, 1997, "Airfoil Boundary-Layer Development and Transition with Large Leading-Edge Roughness", AIAA Journal, vol. 35.

[4] Janiszewska.J, Ramsay.R, Hoffmann.M.J, Gregorek.G.M, 1996, "Effects of Grit Roughness and Pitch Oscillations on the S814 Airfoil", Airfoil Performance Report, Revised (12/99), National Renewable Energy Laboratory, USA.

[5] van Rooij.R. P. J. O. M, Timmer. W. A, 2003, "Roughness Sensitivity Considerations for Thick Rotor Blade Airfoils" ASME Journal of Solar Energy Engineering, vol.125.

[6] Menter.FR, Langtry.RB, Likki.SR, 2006, "A Correlation-Based Transition Model Using Local Variables— Part I: Model Formulation", Journal of Turbomachinery, vol.128.

[7] Tangler J.L and Somers D.M., 1995, NREL airfoil families for hawts. Technical report, NREL.

[8] Corten G.P., 1999, "Insects cause double stall", Symposium on aerodynamics of wind turbines, Stockholm, pp.6-74.

[9] Burton. T, Sharpe. D, Jenkins. N, Bossanyi. E, 2001, " Wind Energy Handbook", John Wiley and Sons, ISBN 0-471-48997-2.

[10] Ren. N, Ou. J, 2009, "Dust effect on the performance of wind turbine airfoils", Journal of Electromagnetic Analysis & Applications, vol.1, pp 102-107